Proceedings of IMECE2008
2008 ASME International Mechanical Engineering Congress and Exposition
October 31-November 6, 2008, Boston, Massachusetts, USA

IMECE2008-67974

ADAPTIVE METHODS FOR NON – LINEAR EMPIRICAL SIMILITUDE METHOD

Srikanth Tadepalli
Department of Mechanical Engineering
The University of Texas at Austin
Austin, TX 78712
512 – 762 – 0247
tsrikanth@mail.utexas.edu

Kristin L. Wood
Department of Mechanical Engineering
The University of Texas at Austin
Austin, TX 78712
512 – 471 – 0095
wood@mail.utexas.edu

ABSTRACT
Several problems in engineering realm pose modeling and simulation difficulty due to severe non – linear behavior and debilitating singular or stiff conditions that act as additional impediments. In many such instances advanced numerical schemes are employed to either relax or simplify the PDE that defines the physical process to obtain reasonable output from the simulation. Digressing from this traditional approach, we present an experimental similitude method in this paper to analyze non – linear systems. Combined with the use of original mapping algorithms, we discuss the benefits of empirical similarity techniques and present a heat transfer example for exposition.

INTRODUCTION
Most technical problems encountered in industrial systems have complex interactions of sub – systems and components unlike conventional problems in the academic world. Analyzing the behavior of a system with a network of components requires multifaceted approximations to reasonably simplify the modeling effort. More often than not, a dominant phenomenon is isolated that captures a major segment of the system response without compromising the integrity of the governing dynamics of the associated physical process. Such a simplification cannot be achieved with considerable ease and requires numerous approximations and assumptions. This feature is more profound in product design, especially in the evolution phase of the product when the geometry is still hypothetical.

When a design needs to be qualified parametrically [Otto et al, 2001], the system has to be evaluated mathematically using a procedure that is both accurate and robust. Such a procedure must also encompass uncertainty indicators and error definitions for the designer to take advantage of to maintain rigorous quality and reliability standards. Keeping in mind that most modern designs are intricate in geometry and are manufactured from multi – material composites or involve multiple material effects, any traditional effort like bond graphs [Karnopp et al, 2006] or Finite Element Methods (FEM) [Becker et al, 1981] necessitate increased graphical and computational effort. The Empirical Similitude Method (ESM) [Cho, 1999] thus provides an alternate evaluation practice that directly combines the physical experimental data with the scaling parameters superseding the need to model the physics of the system *i.e.*, the PDE of the system.

NOMENCLATURE
Xms – Model specimen state vector
Xps – Product specimen state vector
Xm – Model state vector
Xp – Product state vector
F – Form matrix
S – Shape matrix
T – System matrix
k – interval

BACKGROUND INFORMATION
The ESM process derives its premise from the well known Buckingham π theorem where a complex object, *product*, is approximated by a simple yet representative system, *model*, [Langhaar, 1951] that is tested for the parameter of interest [Bridgman, 1931]. These results are then mapped to the actual system using scaling factors between the corresponding geometric and material variables [Skoglund, 1967]. However the scaling accuracy of such transformations depends on the ability to identify all pertinent variables affecting the system and combining them to form the right π groups [Murphy, 1950]. Any indication of increased non – linear effects or time varying behavior negates the robustness of the process even though some progress can still be achieved using higher order approximations [Szirtes, 1998]. The issue compounds when multiple materials interact and boundary or initial conditions assume variations that change with time and space or if the PDE of the system is complex or worse, unknown. Thus arises the need to search for alternate analysis procedures of which ESM is one. ESM thus provides relief by –

- Simplifying the analysis effort by incorporating scaling methods using experimental data thus nullifying the need to generate a PDE of the system dynamics.
- Accurately mapping realistic test information rather than simulating conditions which are unreliable without experimental evidence.

Thus we skip the top – down conventional modeling effort (PDE – Numerical Solution – Experimental Verification) and venture directly into the experimental phase for the required parameter of interest. Shown below is an illustration of the working domains of each process.

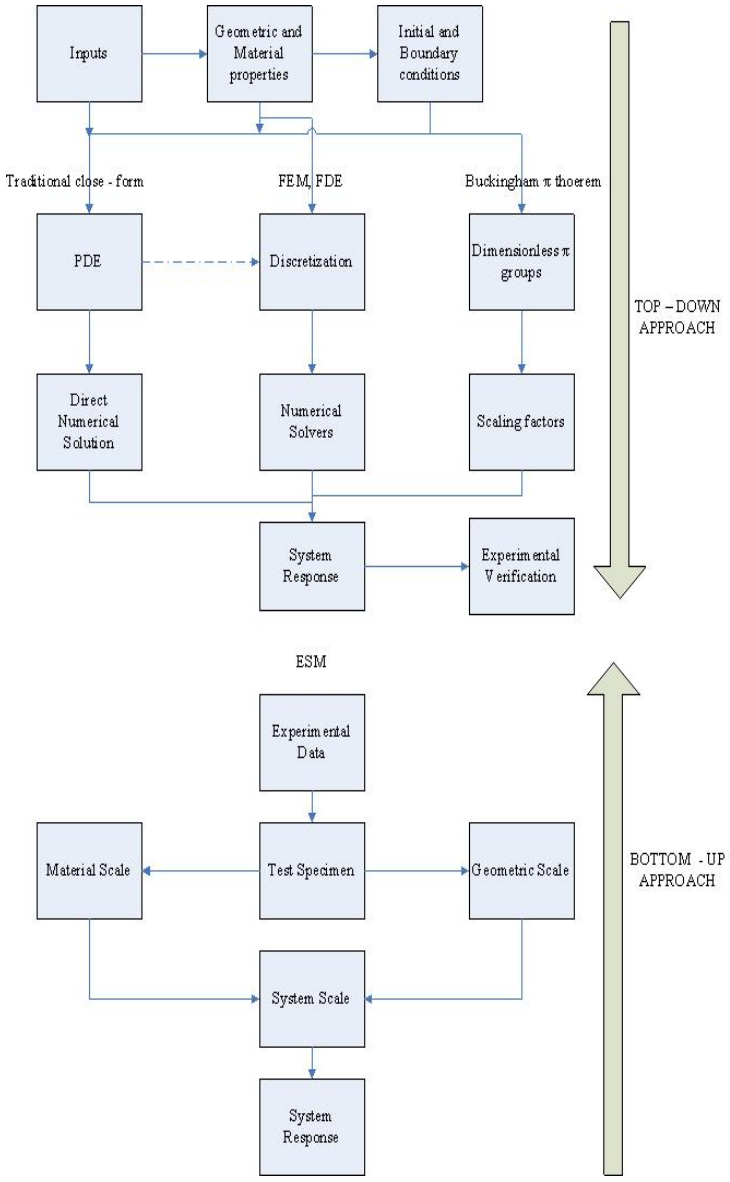

Figure 1. Different Approaches

Note that in all approaches we are interested in estimating hypothetical product behavior. Further, notice that ESM employs intermediate specimen to estimate individual and independent geometric and material scales. The reason for such an assumption stems from the idea that these two scales can be combined to form a comprehensive system scale [Cho, 1999], [Dutson, 2002]. The need for two different scales arises from the fact that has been adhered to in the earlier part of the paper – that of intricate geometries and multi – material effects. In essence, we thus seek a geometry called the *product specimen* (*ps*) that is a simplification of the *product* (*p*) geometry while retaining the same material form, and another geometry called the *model specimen* (*ms*) that is of the same geometry as the *product specimen* but of another material form. Like in the original Buckingham π theorem, the *model* (*m*) is retained to be a scaled version of the *product* but is now of the material form that the *model specimen* is comprised of. In total, we hence have three test specimens instead of just one as in the Buckingham π theorem. To further the benefit of ESM, more often than not, the *model* and the *model specimen* are fabricated using rapid prototyping (RP) processes and are thus impervious to intricate geometric features. Any complexity desired in the *product's* geometry can still be incorporated in the *model* due to rapid prototyping to thus generate a true representation and simplification of the *product*. Similar work using rapid prototyping specimen has been done earlier with considerable success in the industrial arena [Dornfeld, 1995], [Farrar et al, 1994]. Shown below is an illustration of the ESM process using all inherent geometries.

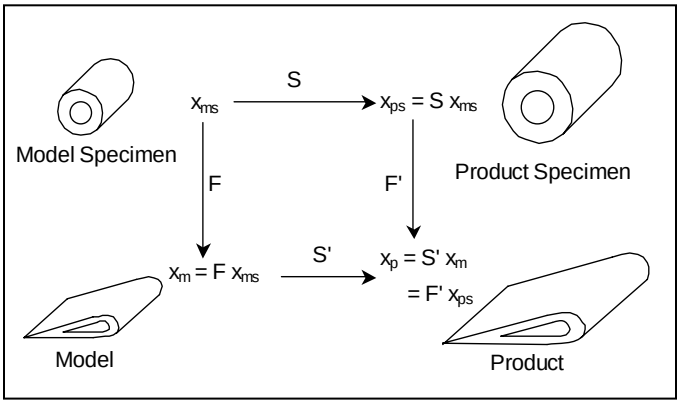

Figure 2. Empirical Similarity Method, Adapted from [Cho, 1999]

The *model* and the *model specimen* combine to indicate the geometric change (the material is constant between the two) referred to as the *form* matrix (*F*) of ESM. The *model specimen* and the *product specimen* couple to capture the material transition (the geometry is constant between the two) referred to as the *scale* matrix (*S*) of ESM. The assumption of independence and symmetry of operation allows us to define $(S \times F) \equiv (F \times S)$ as the *system* matrix that has both geometric

and material information imbibed in it. Such an argument allows for interpreting the *product* response as

$$x_p = Sx_m = (S \times F)x_{ms} \tag{1}$$

where the *scale* equation takes the form given by

$$x_{ps} = Sx_{ms} \tag{2}$$

and the *form* equation is written as

$$x_m = Fx_{ms} \tag{3}$$

Having thus motivated the need, benefits and the working procedure of ESM, we delve into the non – linear methods developed earlier and the current innovations made and illustrate the improvement achieved.

NON – LINEAR METHODS

The first method introduced for analyzing non – linear systems is the *bilinear* ESM [Cho, 1999] where the product state vector is represented using the relation

$$X_p = \frac{uX_m + u_o}{vX_m + v_o} \tag{4}$$

where the constants of the map are derived using the relation

$$X_{ps} = \frac{uX_{ms} + u_o}{vX_{ms} + v_o} \tag{5}$$

The process is a derivative of the Möbius transformation [Grewal, 1998] of a complex number given by

$$w = \frac{az + b}{cz + d},\ ad\text{-}bc \neq 0 \tag{6}$$

The condition $ad\text{-}bc = 0$ characterizes the critical points of the transformation. This transformation is typified by *one – to – one* correspondence of all points in the *z* and the *w* plane. Further, the transformation causes the cross – ratio to hold across all points in the domain, *i.e.*, for any three points in the *z*-plane and the *w*-plane we have

$$\frac{(w_1 - w_2)(w_3 - w)}{(w_1 - w)(w_3 - w_2)} = \frac{(z_1 - z_2)(z_3 - z)}{(z_1 - z)(z_3 - z_2)} \tag{7}$$

Mathematically, the cross ratio should be invariant as the transformed points are fixed and unique for a given set of initial points. Modifying the cross ratio to adapt to ESM, we have,

$$\begin{aligned} u &= z_{ms,2} - z_{ms,1} \\ u_o &= (z_{ms,1} - z_{ms,2})z_{ms,3} \\ v &= z_{ms,2} - z_{ms,3} \\ v_o &= (z_{ms,3} - z_{ms,2})z_{ms,1} \end{aligned} \tag{8}$$

and

$$\begin{aligned} u' &= z_{ps,2} - z_{ps,1} \\ u_o' &= (z_{ps,1} - z_{ps,2})z_{ps,3} \\ v' &= z_{ps,2} - z_{ps,3} \\ v_o' &= (z_{ps,3} - z_{ps,2})z_{ps,1} \end{aligned} \tag{9}$$

The system transformation is now given by

$$T = S \times F = \frac{uX_m + u_o}{vX_m + v_o} \tag{10}$$

such that the *prediction equation* is modified to

$$X_p = \frac{Tv_o' - u_o'}{u' - Tv'} \tag{11}$$

For each triplet of X_m, X_{ms} and X_{ps}, we obtain a single prediction for X_p. Notice that the *bilinear* ESM is inhibited by a potential singularity condition (referred to as the invariance of the process) when $z_{ms,1} = z_{ps,1} = z_{m,1}$ and has limited predictions in its domain *i.e.*, it takes 9 initial points (3 points in each geometry in three successive states) to have a single prediction and hence for *n* states the number of possible predictions is *n* – 2. The final two values need to be generated using extrapolation techniques. The singularity though is removable by a mathematical simplification of the prediction equation. This method is an initial attempt at non – linear ESM [Cho, 1999] and has provided a basis for the development of the next technique that incorporates polynomial mapping of the test data. The second method is the classical *polynomial* ESM method [Cho, 1999] where the product state vector is defined by

$$X_p = \sum_{i=0}^{n} a_i X_m^{\,i} \tag{12}$$

where *n* is the order of the polynomial and the constants a_i's can be derived using the relation

$$X_{ps} = \sum_{i=0}^{n} a_i X_{ms}^{\,i} \tag{13}$$

In this case, the system transformation is given by

$$T = X_m X_{ms}^{+} \tag{14}$$

where $X_{ms}^{+} = (X_{ms}^{*} X_{ms})^{-1} X_{ms}^{*}$ is the pseudo – inverse of X_{ms} and X_{ms}^{*} is the conjugate transpose of X_{ms} [Albert, 1972]. The prediction equation in this case is written as

$$X_p = TX_{ps} \tag{15}$$

where we pick only the second column of the resulting matrix for consideration [Cho, 1999]. Notice that the *polynomial* ESM does not suffer from the singularity drawback but the biggest impediment to the process is to figure out the right order of the polynomial *n* to use. Conventionally, the method has been used where the order, starting from 2, has been incremented in steps of 1 and the error at the end of each step compared to estimate the "best" fit. The inherent limitation of this process is the unavailability of the (hypothetical) *product* data to estimate errors which then inhibits the use of the correct order of the polynomial. Based on these constraints, the requirements for a novel system include –

i) Does not have any singularity conditions.

ii) Provides an accurate estimate of what the best order of the fit is.
iii) Provides flexibility of using alternate methods in intermediate intervals.

While the first two conditions are apparently intuitive, we explain the third condition for lucidity. The two methods presented do not complement each other in the sense that one method cannot be used in conjunction with the other. In a given working domain, a designer needs to choose one of the methods but can never use both either partially or to complement the other. Thus, both methods lack the flexibility to incorporate other methods into their working process. Three different methods that are developed to address the issues discussed above include –

a) Adaptive Polynomial ESM
b) Adaptive Exponential Regression ESM
c) Adaptive Power Regression ESM

Notice the emphasis given to adaptiveness in the three methods. This is done to reap the benefits of discretization of the working interval that allows piecewise (interval specific) error check. These errors and their significance, and their implication in adaptive ESM methods are discussed later in the paper. Since we discretize the working interval into several sub – intervals, we can adapt the polynomial order and the interval width and combine individual interval solutions to form the system response by coupling the points at the end of each interval using the arithmetic mean of the left and right intervals. This is again illustrated in the next section.

NOVEL NON – LINEAR METHODS: MATHEMATICAL DEVELOPMENT

To improve non - linear ESM, three new methods have been proposed in the previous section. These methods account for the identified restrictions of prior techniques and expand the process by imbibing robustness into the evaluation procedure. This robustness is brought on by the adaptive nature and singularity isolation characteristics of the methods. These techniques still have to either better or maintain the accuracy margins achieved by the earlier two methods. We present the analytical description and the working procedure of each process.

All the methods rely on the power of adaptivity where the entire working range is discretized into several intervals and each interval is then scaled individually, a process that allows for comparison of experimental and estimated data so that the right order of the polynomial can be established without any ambivalence. Further, the added advantage of the procedure is the notification of potential error induced when orders of polynomials greater the required order is used. This latent limitation in *polynomial* ESM is shown using an example later on. Adaptive methods however have the ability to pick the next data point and the next order when the estimated interval error for a given order is not in the acceptable margin. Hence in the limiting condition

$$\textit{Adaptive Polynomial}\ \text{ESM} \rightarrow \textit{Polynomial}\ \text{ESM as } k \rightarrow 1$$

k being the number of intervals. The current focus though is to demonstrate the improved estimation process while adhering the stringent error margins. In the adaptive polynomial ESM process, the estimation is still based on a curve fit given by

$$\left[X_p\right]_k = \left[\sum_{i=0}^{n} a_i X_m^{\,i}\right]_k \tag{16}$$

where *n* is the order of the polynomial and the constants a_i's still derived using the relation

$$\left[X_{ps}\right]_k = \left[\sum_{i=0}^{n} a_i X_{ms}^{\,i}\right]_k \tag{17}$$

However, the notable difference is the use of the interval *k* and hence individual and independent maps are produced to obtain *scale* and *form* transformations. Collecting the individual transformations produces the required system *scale* and *form* transformation which is then used for prediction purposes. The system transformation is now modified to

$$T_k = \left(X_m X_{ms}^{+}\right)_k \tag{18}$$

and the prediction equation assumes the form

$$\left(X_p\right)_k = T_k \left(X_{ps}\right)_k \tag{19}$$

In the adaptive exponential regression ESM process, the prediction is based on the relation given by

$$\left[\ln(X_p)\right]_k = \left[\ln(a) + \ln(b) X_m\right]_k \tag{20}$$

where *k* is the interval and the constants *a* and *b* are derived using the relation

$$\left[\ln(X_{ps})\right]_k = \left[\ln(a) + \ln(b) X_{ms}\right]_k \tag{21}$$

Hence in a given interval *k*

$$\ln a = \left(\frac{X_{ms,1} X_{ms,2}}{X_{ms,1} - X_{ms,2}}\right) \ln\left[\frac{\left(X_{ps,1}\right)^{\frac{1}{X_{ms,1}}}}{\left(X_{ps,2}\right)^{\frac{1}{X_{ms,2}}}}\right]$$
$$\ln b = \left(\frac{1}{X_{ms,1} - X_{ms,2}}\right) \ln\left(\frac{X_{ps,1}}{X_{ps,2}}\right) \tag{22}$$

Notice that we need just two points to make a prediction that is unique to the interval of interest and since $X_{ms,1}$ and $X_{ms,2}$ are always unique, the condition of singularity is completely avoided. In the limiting condition for a measurement point *i*, if $X_{ms,i} \rightarrow 0 \Rightarrow a \rightarrow X_{ps,i}$ and *b* is an arbitrary constant and therefore a free choice (1 DOF). Here we are discounting the necessity to model the other extremum at ∞ as typical

mechanical systems and products do not have undefined, indeterminate or infinitely large values for common parameters. Hence the process is mathematically stable and further allows comparison of experimental and estimated values of X_{ps} in each interval. This contrast translates to important scaling information regarding the efficiency of the technique. In the adaptive power regression ESM process, the prediction is based on the relation given by

$$\left[X_p\right]_k = \left[aX_m^b\right]_k \tag{23}$$

where *k* is the interval and the constants *a* and *b* are derived using the relation

$$\left[X_{ps}\right]_k = \left[aX_{ms}^b\right]_k \tag{24}$$

In this case just three points are needed to make a prediction that is unique to the interval of interest. Hence, for a set of measurement points in the *model specimen* and the *product specimen* given by $\{X_{ms,1}, X_{ps,1}\}$ and $\{X_{ms,2}, X_{ps,2}\}$, we can uniquely fit a curve of the form specified (see Equation (23)) with well determined values for the constants *a* and *b*. In the limiting condition for a measurement point *i*, if $X_{ps,i} \to 0 \Rightarrow a \to 0$ for non – trivial values of $X_{ms,i}$ and, *b* is again an arbitrary constant and therefore a free choice (1 DOF). Here again we ensure mathematical stability and discount the necessity to model the other extremum at ∞ for reasons mentioned earlier. Note that in all these methods we have several interval mappings and predictions that need to be coupled to generate a system level response. Since an interval is characterized by two directions, we use the arithmetic mean at the junction so that continuity of the solution is maintained.

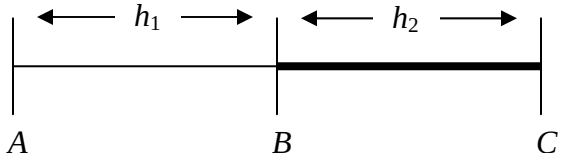

Figure 3. Estimation at the Junction

If in the interval h_1 the predictions made at points *A* and *B* are X_A and X_{B^-} and similarly in the interval h_2 the predictions made at points *B* and *C* are X_{B^+} and X_C, then in order to maintain continuity of the solution, the elemental solutions are modified to

$$\begin{aligned} X_A^* &= X_A \\ X_B^* &= \frac{X_{B^-} + X_{B^+}}{2} \\ X_C^* &= X_C \end{aligned} \tag{25}$$

We now make a comparison of methods to understand the intricacies of each scheme.

Table 1. Comparison of Methods

Technique	Singularities	"Right" Order of Polynomial
Polynomial ESM	No	Unknown
Bilinear ESM	Yes	1
Adaptive Polynomial ESM	No	Known
Adaptive Exponential Regression ESM	No	Order not required
Adaptive Power Regression ESM	No	Order not required

The biggest and single most important innovation in the development of these processes is their ability to interact and complement each other – a feature that was sorely missing in the two earlier methods. Consider a situation where the working domain is discretized into five intervals. The flexibility of these methods allows them to be used together implying that the adaptive polynomial ESM could be used in the first interval while the adaptive exponential regression ESM takes over in the next and the adaptive power regression ESM thereafter. Remember that such a decision needs to made based on predicted error values that are expected in each method for each interval. Based on the numerical estimates of the error that each method generates in each interval, we can mix and match methods to generate a composite graph of adaptive methods. This phenomenon represents true adaptivity where interval length, polynomial order and scaling method are all combined. Before we present the robustness of the adaptive methods in terms of accuracy – the single most important criterion for selection, we introduce the error definitions used for the analysis and the means to estimate them in the next section.

ERROR DEFINITONS

Assume that we are interested in establishing the *scale* matrix or transformation in the ESM process. If both involved geometries *i.e.*, *model specimen* and *product specimen* have $n+1$ points in their working domain, let P_{ms} and P_{ps} be the set of points (measurement values) that are being mapped. Then

$$\begin{aligned} P_{ms} &= \left\{P_i^{ms}\right\}_{i=0}^n \\ P_{ps} &= \left\{P_i^{ps}\right\}_{i=0}^n \end{aligned} \tag{26}$$

and if the points are numbered as $\{y_j\}_{j=0}^n$ in both geometries such that $y_0 = 0$ and $y_n = R$ (characteristic length of the working domain), we then have *n* intervals each of length $h = \frac{R}{n}$. Further, we wish 1 – 1 correspondence between the

values of the parameter in the two geometries. Hence the points of evaluation are defined such that

$$y_i^{ps} = \lambda y_i^{ms}\ ;\ \lambda = \frac{R_{ps}}{R_{ms}} \tag{27}$$

For each of the points *i* in both geometries we have an associated value for the parameter of interest P_i. The task now is to establish the functional form that uniquely associates P_i^{ps} with P_i^{ms}. Hence for the set of ordered pairs $\left\{\left(P_i^{ms}, P_i^{ps}\right)\right\}_{i=0}^{n}$ we need to establish a curve that enforces a C^0 continuous explicit relationship between P_i^{ps} and P_i^{ms} since we have only discrete nodal point values in the evaluation of the material transform (*scale*) that estimates the functional form of the net change in the material properties between the *model specimen* and the *product specimen.* Let $f(y)$ be that curve. Then the subscript *e* denoting estimated value,

$$P_{i,e}^{ps} \approx f(y) P_i^{ms} \tag{28}$$

Since the dimension *R* can assume values that are fairly large, we discretize the length into intervals as defined earlier. Instead of having a single transformation over the entire distance, we map individual intervals of length *h* for closer fits.

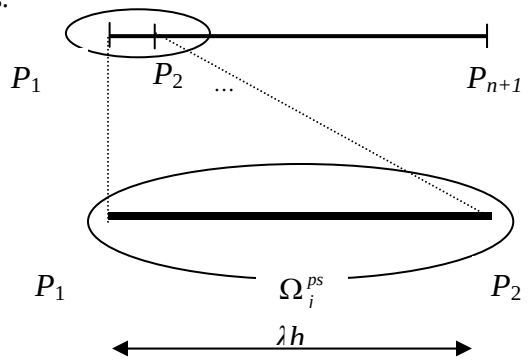

Figure 4. Elemental Evaluation

Hence if Ω_j^{ms} and Ω_j^{ps} are the corresponding intervals, then we fit

$$P_{i,e}^{ps} \approx f_i(y) P_i^{ms} \tag{29}$$

where the point of evaluation $i \in \Omega_j$ in both intervals while enforcing the scalar constraint λ from above. Hence defining the L^2 norm for error estimation in each interval mapping,

$$\begin{aligned} &\left\|e_j\right\|_{L^2} = \left\|\sum e_i\right\|_{L^2} = \left\|P_i^{ps} - P_{i,e}^{ps}\right\|_{L^2} \\ &\forall\, i \ni y_i \in \Omega_j = \left\{y_i \mid y_a \le y_i \le y_b\right\}; e_i = e\left(y_i\right) \end{aligned} \tag{30}$$

where y_a is the start point of the interval and y_b is the end point of the interval and $\left|y_b - y_a\right| = h$. Since we need continuous definitions for $P_{i,e}^{ps}$ and P_i^{ms} for evaluating the L^2 norm which are not available, a discrete estimation is formulated using 2 – point Gauss quadrature such that

$$\begin{aligned} \left\|\bullet\right\|_{L^2} &\left[= \int_{y_a}^{y_b} \left(\left\|\bullet\right\|\right)^2 dy \right]^{\frac{1}{2}} = \left[\sum \int_{y_i}^{y_{i+1}} \left(\left\|\bullet\right\|\right)^2 dy \right]^{\frac{1}{2}} \\ &= \left[\sum \left\{\left(\left\|\bullet\right\|\right)^2 (y_i) + \left(\left\|\bullet\right\|\right)^2 (y_{i+1})\right\}\right]^{\frac{1}{2}} \\ &\forall\, i \ni y_i \in \Omega_j = \left\{y_i \mid y_a \le y_i \le y_b\right\} \end{aligned} \tag{31}$$

Defining average global error across all intervals, we have

$$\varepsilon_g = \frac{\sum_{j=1}^{n} e_j h_j}{L} \tag{32}$$

Note that the value of ε_g depends on the degree of the polynomial *p* and the length of the interval *h* and hence varies according to the *h – p* constraint [Becker et al, 1981]. We choose the L^2 norm as it represents the root mean square (RMS) error, an indicator to account for possible generation of negative errors. The objective now is to show that the error in the L^2 norm is convergent with a negative slope. Detailed below is the algorithm for the adaptive polynomial ESM. Similar heuristics can be setup for the other two adaptive methods as well with corresponding characteristics.

ALGORITHM

Step 1: *Set* $\varepsilon \to tol$

(Initial value of error to be equal to some fixed finite tolerance)

Step 2: *Set* $m \to 2$, *Set* $n \to m$

(Initial search index of polynomial set to degree 2. This implies that a quadratic polynomial is fitted in each interval. Further, we have 3 DOF and hence each interval has three nodes).

Step 3: *Set* $(\overline{z_i}) \to \{x_i, y_i\}$, the end points of each interval.

(If the material is isotropic throughout, then each interval is of uniform length else the interval length is determined by the end points located exactly where a change in material property occurs)

Step 4: *Set* $h \rightarrow \frac{L}{xn}$

(For isotropic material, the element length is forced to a value equal the ratio of a characteristic length and a multiple of the degree of the polynomial where $x \varepsilon N$)

Step 5: *Fit* $\phi_i(\overline{z_j}) \rightarrow \sum_{j=0}^{n+1} a_j z^j$

(The curve that fits the distribution of values at points $(\overline{z_i}) \rightarrow \{x_i, y_i\}$ between the two geometries; *z* represents the value of the parameter of interest at $\{x_i, y_i\}$)

Step 6: *Estimate local truncation error* $\varepsilon_{l,i} \rightarrow \left|\phi - \phi_i\right|$

(L^2 norm)

Step 7: *Set* $i \rightarrow i+1$

Step 8: *Set* $\Xi \rightarrow tol$

Step 9: *Repeat Step 5 and Step 6 for all intervals and estimate global error*

Do $\phi_i(\overline{z_j}) \rightarrow \sum_{j=0}^{n} a_j z^j$

$\varepsilon_{l,i} \rightarrow \left|\phi - \phi_i\right|_{L^2}$

$\varepsilon_g \rightarrow \frac{\sum_{i=1}^{xn} \varepsilon_{l,i} h_i}{L}$

While $i \le xn$

such that

$\left|\phi_{i-1}(\overline{z_{n+1}}) - \phi_i(\overline{z_0})\right| \le \Xi$

Step 10: *If* $\left|\varepsilon_g\right|_k \le \Xi$ and $\left|\varepsilon_g\right|_{k+1} < \left|\varepsilon_g\right|_k$

Print Convergence obtained

Print x, n

Print $\phi_i(\overline{z_j}) \rightarrow \sum_{j=0}^{n+1} a_j z^j \ \forall i$

Print $\varepsilon_g \rightarrow \frac{\sum_{i=1}^{xn} \varepsilon_{l,i} h_i}{L}$

End

Else

$x \rightarrow x+1$

Repeat Steps 4 through 9

While $x \le n$

Step 11: *If* $x = n$ *and* $\left|\varepsilon_g\right| > \Xi$

$n \rightarrow n+1$

Repeat Steps 4 through 10

While $n \le m^2$

Step 12: *If* $n = m^2$ *and* $\left|\varepsilon_g\right| > \Xi$

Set $y \rightarrow 1$

$\Xi \rightarrow \Xi + y\Xi$

$y \rightarrow y+1$

Repeat Steps 4 through 11

While $\Xi \le 0.05$

Step 13: *If* $y = 100$ *and* $\left|\varepsilon_g\right| > \Xi$

Print Convergence not obtained

We have thus far developed the means to carry out prediction based on sound mathematical principles. In the next section, we apply all the methods to a heat transfer example and complete the much required error analysis.

NUMERICAL EXAMPLE – HEAT TRANSFER PROBLEM

In this numerical experiment, the temperature distribution of a regular kitchen skillet is predicted based on chosen specimen geometry (see Figure 5) for a constant heat source applied to the base. The skillet is copper bottom steel geometry with shape as shown below. The specimen geometry chosen is a perfect hemisphere made from nylon. Note that the flux applied to the geometries changes from surface in the *product* and the *model* to a point load in the *model specimen* and the *product specimen*. This creates a distortion in input conditions that should affect prediction but ESM is shown to have a minimal effect in such conditions. Further, the effect of non – linearity is brought on by the convective currents that cool the appliances down while being used for cooking. The results of analysis are plotted below.

Figure 5. Skillet and Skillet Specimen

The geometries are analyzed using SolidWorks™ software for steady – state temperature values at discrete points starting from the center of the base.

Table 2. Measurement Data

Measurement	T_{ms}	T_{ps}
1	89.1900	90.0700
2	86.4500	86.8400
3	83.6600	82.5800
4	79.4500	78.5700
5	76.4300	76.5500
6	72.7800	72.2500
7	69.4500	68.5700
8	66.6500	65.4400
9	62.1200	61.6400
10	58.8400	57.3800
11	54.5100	54.0400

In the first phase, we estimate the *scale* transformation matrix in the first interval for all the adaptive methods using the relations provided before. The values come out to be

$$S_{AP} = [-500.355 \quad 12.2333 \quad -0.0629384]$$
$$S_{AER} = [1.013417613 \quad 27.43522153] \qquad (33)$$
$$S_{APR} = [53985.4 \quad 0.0021489]$$

Using these *scale* matrix values we predict the temperatures for the *product specimen* and the results are shown below for all the adaptive methods. Note that all the adaptive methods provide a near perfect estimate with change observed only in the insignificant fourth decimal. Hence, the second order is persisted with for the entire evaluation for the adaptive polynomial ESM process and likewise we make similar estimations for the other two adaptive processes by establishing the constants and then making the prediction.

Table 3. Predicted values for T_{ps}

Adaptive Polynomial (2nd Order)	Exponential Regression	Power Regression
90.07	90.07	90.07
86.84	86.84	86.84
82.58	82.58	82.58
78.57	78.57	78.57
76.55	76.55	76.55
72.25	72.25	72.25
68.57	68.57	68.57
65.44	65.44	65.44
61.64	61.64	61.64
57.38	57.38	57.38
54.04	54.04	54.04

Once the *scale* matrix has been established and verified, we generate the *form* matrix using the measurement data between the *model* and the *model specimen*. Using the two matrices and the prediction equations for the respective methods, the product state vector is estimated. The results are shown below. Notice that the adaptive methods compare positively with *bilinear* ESM in terms of error margins and are comparable to *polynomial* ESM (see Figure 7). Notice also the trend or the distribution of the temperature (see Figure 6) is commensurate with the actual distribution for all techniques. This is another feature of the adaptive methods that allow them to 'self – correct' in order to maintain the trend pattern. Even though adaptive methods require more effort, the enterprise pays off in terms of error reduction. The only variable that changes in this experiment is time and hence the adaptive algorithms treat this as an independent variable.

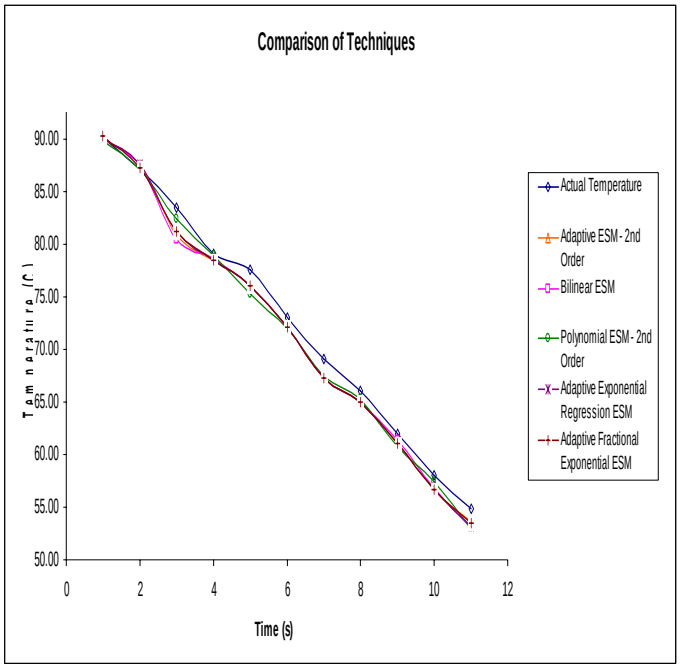

Figure 6. Prediction Plot

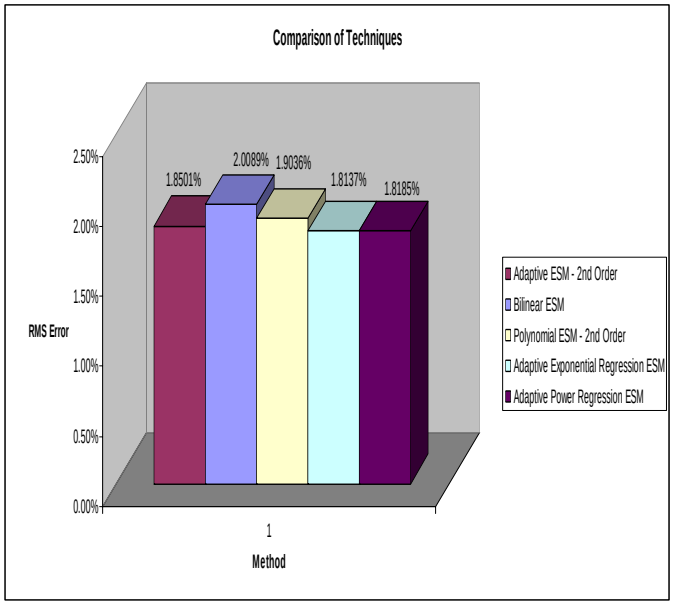

Figure 7. Error Comparison

Table 4. Comparison of Methods

	Method	RMS Error
1	Polynomial ESM	1.9036%
2	Bilinear ESM	2.0089%
5	Adaptive Polynomial ESM	1.8501%
4	Adaptive Power Regression ESM	1.8185%
3	Adaptive Exponential Regression ESM	1.8137%

Further, notice from the graph below that the objective of establishing convergent behavior has been achieved where the error values have decreased with the newer methods. There is now flexibility of choosing the method that most easily fits into the parametric modeling efforts of the designer so that computational effort is optimized with time constraints.

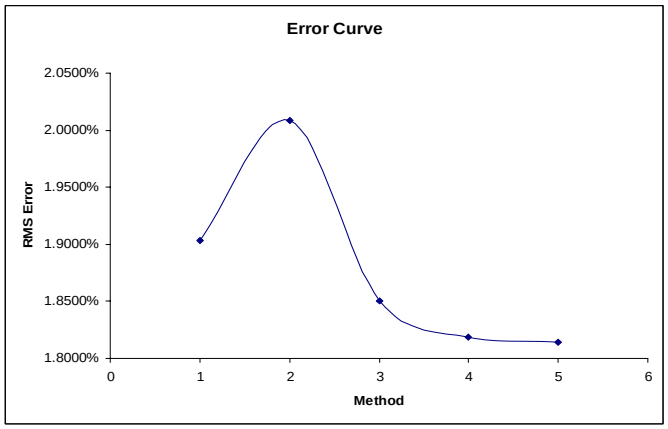

Figure 8. Error Graph

SUMMARY

The ESM process has been discussed with the need and justification provided for experiential similitude over the conventional Buckingham π theorem. We have provided a means for empirical similarity in product design parametric analysis using three novel adaptive methods all of which have been complemented with thorough analytical descriptions, rigorous error definitions and simulation parameters. A further discussion on the potential benefit of using adaptive methods over the conventional *bilinear* and *polynomial* ESM methods has been offered. We summarize the analysis by presenting the adaptive processes from a data flow perspective.

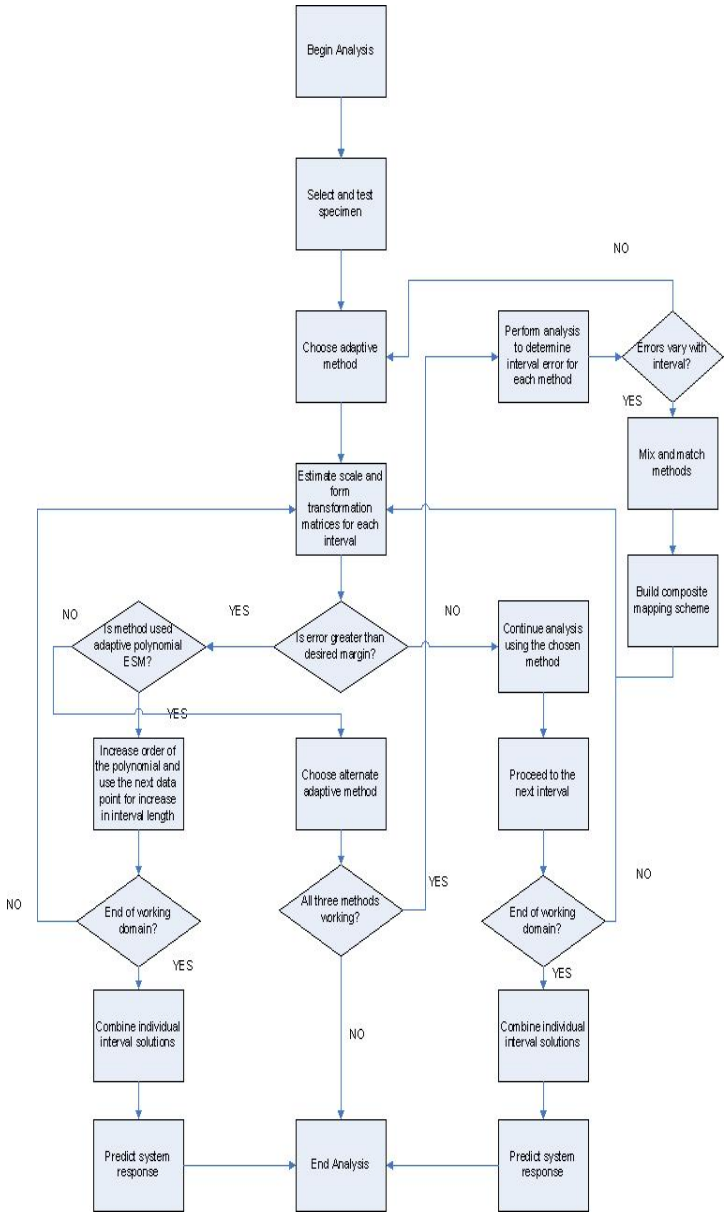

Figure 9. Non – linear ESM Flow Chart

CONCLUSIONS AND FUTURE WORK

The non – linear ESM process has been developed to a point where it can be directly incorporated into mechanical design work for numerical and analytical validations of future designs or re – designs. As is illustrated from the error graphs the adaptive methods developed have been shown to be highly accurate and robust and present an interesting choice for mathematical reasoning in parametric design process selection. Several intermediate innovations have been described including establishing the right polynomial order, developing methods that do not require orders, ability to use methods that interact with each other and convergence norms. All this has been achieved while maintaining or bettering the accuracy margins of earlier methods. Future developments in the field of ESM must incorporate these trends for a comprehensive evaluation for non – linear systems.

References:

[1] Albert, A., 1972, *Regression and the Moore – Penrose Pseudoinverse*, Academic Press.

[2] Baker, W. E., Westine, P. S., Dodge, F. T., 1991, *Similarity Methods In Engineering Dynamics: Theory And Practice of Scale Modeling*, Elsevier.

[3] Becker E. B., Carey, G. F., Oden, J.T., 1981, *Finite elements*, Prentice-Hall, Englewood Cliffs, NJ.

[4] Bridgman, P. W. 1931, *Dimensional Analysis*, Yale University Press, New Haven.

[5] Cho, U., and Wood, K., 1997, "Empirical Similitude Method for the Functional Test with Rapid Prototypes," *Proceedings of the Solid Freeform Fabrication Symposium*, Austin TX, September, 1997, pp. 559 – 567.

[6] Cho, U., Wood, K. L., and Crawford, R. H., 1998b, "Novel empirical similarity method for the reliable product test with rapid prototypes," *Proceedings of DETC*, Atlanta, GA, September 13 – 16, 1998.

[7] Cho, U., Wood, K. L., and Crawford, R. H., 1998, "Online Functional Testing with Rapid Prototypes: a Novel Empirical Similarity Method," *Rapid Prototyping Journal*, 4, No. 3, pp. 128 – 138.

[8] Cho, U., 1999, *Novel Empirical Similarity Method for Rapid Product Testing and Development*, Doctoral dissertation, The University of Texas at Austin.

[9] David, F. W., Nolle, H., 1982, *Experimental Modelling In Engineering*, ButterWorths.

[10] Dornfeld, W. H., 1995, *Direct Dynamic Testing of Scaled Stereolithographic Models*, Sound and Vibration, August, 12 – 17.

[11] Dutson, A.J, 2002, *Functional Prototyping Through Advanced Similitude Techniques*, Doctoral dissertation, The University of Texas at Austin.

[12] Farrar, C. R., Baker, W. E., Dove, R. C.,1994, *Dynamic Parameter Similitude for Concrete Models*, ACI Structural Journal, Title No. 91 – S10, January – February, 90 – 98.

[13] Grewal, B.S., 1998, *Higher Engineering Mathematics*, Khanna Publishers, Delhi, India.

[14] Hart, G.W., 1995, *Multidimensional Analysis*, Springer – Verlag.

[15] Incropera F.P., 2007, *Fundamentals of heat and mass transfer*, 6th ed, John Wiley, Hoboken, NJ.

[16] Karnopp, D.C., Margolis, D.L., Rosenberg, R.C., 2006, *System dynamics*: *modeling and simulation of mechatronic systems*, 4th ed., John Wiley & Sons, Hoboken, NJ.

[17] Kendell, A. A., 1988, *An introduction to numerical analysis*, 2nd edition, Section 8.9, John Wiley and Sons.

[18] Edited by Klamkin, Murray S., 1987, *Mathematical Modelling: Classroom Notes In Applied Mathematics*, SIAM.

[19] Langhaar, H. L., 1951, *Dimensional Analysis and Theory of Models*, John Wiley & Sons, New York.

[20] Linz, P., 1979, *Theoretical numerical analysis: an introduction to advanced techniques*, Wiley, New York.

[21] Mordecai, Avriel, 2003, *Nonlinear Programming: Analysis and Methods*, Dover Publishing.

[22] Murphy, G., 1950, *Similitude in Engineering*, The Ronald Press Company, New York.

[23] Otto, K. N., Wood, K.L., 2001, *Product Design – Techniques in Reverse Engineering and New Product Development*, Prentice Hall, Upper Saddle River NJ.

[24] Rayleigh, 1915, *The Principle of Similitude*, Nature, No. 2368, Vol. 95, 66 – 68.

[25] Schnittger, J. R., 1988, *Dimensional Analysis in Design*, Journal of Vibration, Acoustics, Stress and Reliability in Design, Vol. 110, January – February, 401 – 406.

[26] Skoglund, V.J., 1967, *Similitude – Theory and Applications*, International Textbook Company, PA.

[27] Szirtes, T., 1998, *Applied Dimensional Analysis and Modeling*, McGraw – Hill, New York.

[28] Szücs, E., 1980, *Similitude And Modelling*, Elsevier.

[29] Taylor, E. S., 1974, *Dimensional analysis for engineers*, Clarendon Press, Oxford.

[30] Wood, J. J., and Wood, K. L. 2002b. "Empirical Analysis using Advanced Similarity Methods," *Proceedings of DETC*, Montreal, Canada, 2002, pp. 429 – 438.